

UNIOSUN Journal of Engineering and Environmental Sciences. Vol. 7 No. 1. March. 2025

Significance of Multiple Slip and Induced Magnetic Field on Unsteady MHD Nano-Fluid Stagnation-Point Flow over a Stretching Wedge

Akinrinmade, V. A. and Kolawole, M. K.

Abstract This study investigates the unsteady magnetohydrodynamic (MHD) flow of a nano-fluid over a stretching wedge, emphasizing the effects of multiple slip conditions and induced magnetic fluid dynamics. The presence of slip at the boundary is modeled to account for non-local effects, enhancing the understanding of fluid behavior in micro- and nano-scale applications. The governing equations are formulated and solved using numerical techniques to analyze the flow characteristics, heat transfer and induced magnetic fields. Results reveal that the inclusion of multiple slip conditions significantly alters the velocity and temperature profiles, while the interaction between the magnetic field and the nano-fluid properties leads to variations in the flow stability and thermal conductivity. The findings provide valuable insights for optimizing industrial processes involving magnetically controlled nano-fluids with potential applications in cooling systems, material processing and biomedical devices.

Keywords: Magnetohydrodynamics (MHD), Nanoparticles, Nonlinear stretching wedge, multiple slips, Non-uniform heating.

I. Introduction

The study of magnetohydrodynamics (MHD) has gained prominent attention due to its wideranging applications in engineering technology, particularly in processes involving electrically conducting fluids [1]. The interaction between magnetic fields and fluid motion is optimizing various industrial crucial in applications, such as cooling systems, material processing, and electromagnetic pumps. Recent advancements nanotechnology in introduced nano-fluids, which are colloidal suspensions of nanoparticles in a base fluid. These nano-fluids exhibit enhanced thermal properties and improved heat transfer capabilities, making them ideal for use in MHD applications [2, 3]. In this context, the stagnation

Akinrinmade, V. A., Kolawole, M. K.

(Department of Mathematical Sciences, Osun State University, Osogbo. Nigeria)

Corresponding Author:: mutairu.kolawole@uniosun.edu.ng

point flow over a stretching wedge serves as a fundamental model to explore the behavior of MHD nano-fluids. This scenario is particularly relevant for processes where materials are continuously drawn through a deforming surface, such as in extrusion and drawing operations. The introduction of slip boundary further complicates the conditions dynamics, allowing for more realistic modeling of fluids in contact with solid surfaces [4]. Slip conditions can arise due to various factors, including molecular effects at small scales and surface roughness, which can significantly influence the flow characteristics. Additionally, the effects of induced magnetic fields in MHD systems are critical, as they can alter the velocity and thermal profiles of the fluid, impacting stability and performance by [5]. Understanding the interplay between multiple slip effects and induced magnetic fluid dynamics is essential for

accurately predicting the behavior of nano-fluids under unsteady conditions [6, 7]. This study aims to investigate the significance of multiple slip conditions and induced magnetic effects on the unsteady MHD nano-fluid stagnation point flow over a stretching wedge in [8]. By analyzing the governing equations and employing numerical techniques, we seek to provide a comprehensive understanding of the flow characteristics, potential thermal behavior and the optimizing MHD applications in industrial settings by [9-11]. The findings will contribute to the growing body of knowledge on nano-fluids and their application in advanced MHD systems, paving the way for innovative solutions in various engineering fields.

II. Materials and Methods

We assume a Falkner Skan of an flow incompressible unsteady tangent hyperbolicnanofluid over a faster/slower stretching wedge in light of an applied magnetic field along with activation energy and magnetic field. The Reynolds number is considered very small, and prompted magnetic field would ignore. The fluid is assumed to be Newtonian, electrically conducting and its property variations due to temperature and induced magnetic field are limited to fluid density. Also, the induced magnetic field is assumed to be either also contribute to the fluid flow properties. Let the x —axis be taken along the direction of plate and y-axis normal to it. If u, v, T and $B_i, i = 1,2$ are the fluid *x*-component of velocity, y -component of velocity, temperature and induced magnectic respectively. Further, we considered that fluid flow is caused by stretching wedge with the velocity

$$u_w(x,t) = \frac{bx^m}{1-ct} \tag{1}$$

The free stream velocity for the current problem is

$$u_e(x,t) = \frac{ax^m}{1 - ct} \tag{2}$$

where m, a, b, c are positive constants with $0 \le m \le 1$, and ct < 1. The angle of the wedge is supposed to be

$$\Omega = \pi \beta$$
, where $\beta = \frac{2m}{1+m}$ (3)

Symbolizes the wedge angle parameter. From the perspective of a positive value of β (β > 0) provides acceleration to the fluid flow and value of β (β < 0) retardation. Additionally, $\beta = 0$ (i.e., m =0) corresponds to boundary layer flow over a horizontal flat plate and $\beta = 1$ (i.e., m =1) relate to boundary layer flow near the stagnation point of a vertical flat plate. Further, we assume that (concentrations, temperature) at the wedge surface (C_w, T_w) are higher than the ambient (concentrations, temperature) i.e., (C_{∞}, T_{∞}) that is , $C_w > C_{\infty}$, and $T_w > T_{\infty}$. The Cartesian coordinates (x, y) is utilized with x correspond coincides with the surface of the wedge and y perpendicular to it, and $y \ge 0$ is the fluid occupied region.

Also, the fluid binary reaction under the influence of moving flat surface, buoyance forces and magnetic field occurs in a permeable device with isothermal boundary layer. The chemical mixture for a single exothermic reaction with continuous particle collision is propelled by chemical heat generation and chemical kinetics.

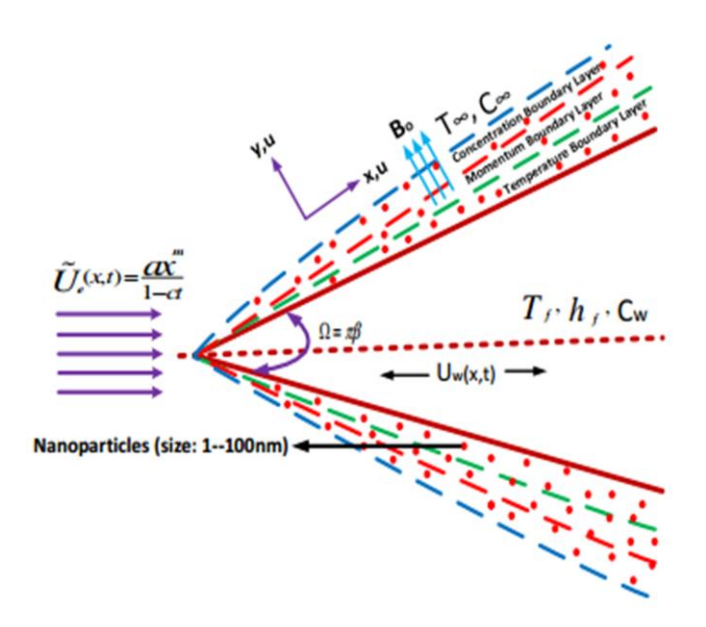


Figure 1: Schematic Flow of Distribution

conservation mass and magnetic balance are given as:

Continuity equations for mass and magnetic field

$$\frac{\partial u}{\partial x} + \frac{\partial u}{\partial y} = 0$$

$$\frac{\partial B_1}{\partial x} + \frac{\partial B_2}{\partial y} = 0$$
(4)

Momentum Equation

$$\frac{\partial u}{\partial t} + u \frac{\partial u}{\partial x} + v \frac{\partial u}{\partial y} = u_{\ell} \frac{du_{\ell}}{dx} - \left[\frac{\mu_{nf}}{\rho_{nf}} \left(1 + \frac{1}{\gamma} \right) + \sqrt{2nf} \left(\frac{\partial u}{\partial y} \right) \right] \frac{\partial^{2} u}{\partial y^{2}} \pm \frac{g}{\rho_{nf}} \left(\frac{k_{1}}{v} \right) |\hat{u}| (u - U)$$

$$- \frac{\mu_{\ell}}{4\pi \rho_{nf}} \left(B_{1} \frac{\partial B_{1}}{\partial x} + B_{2} \frac{\partial B_{1}}{\partial y} - B_{0} \frac{dB_{0}}{dx} + \frac{g}{\rho_{nf}} \left[\beta_{r} (T - T_{\infty}) + \beta_{c} (C - C_{\infty}) \right] \right)$$
(5)

Induced Magnetic Field Equation

$$\frac{\partial B_1}{\partial t} + u \frac{\partial B_1}{\partial x} + v \frac{\partial B_1}{\partial y} = B_1 \frac{\partial u}{\partial x} + B_2 \frac{\partial u}{\partial y} + \mu_{\circ} \frac{\partial^2 B_1}{\partial y^2} - \frac{k_{nf}}{(\rho c_p)_{nf}} \frac{\partial q_r}{\partial y^r}.$$
(6)

Energy Transfer Equation

$$\frac{\partial T}{\partial t} + u \frac{\partial T}{\partial x} + v \frac{\partial T}{\partial y} = \frac{k_{hnf}}{(\mathbf{z}_{p})_{hnf}} \frac{\partial^{2} T}{\partial y^{2}} + N \left[D \frac{\partial T}{\partial y} \frac{\partial C}{\partial y} + \frac{D_{T}}{T_{\infty}} \left(\frac{\partial T}{\partial y} \right)^{2} + \left(1 + \frac{1}{\gamma} \left(\frac{\partial u}{\partial y} \right)^{2} \right) \right] + \frac{1}{\partial (c_{p}\rho)_{nf}} \left(\frac{\partial B_{1}}{\partial y} \right)^{2} + \frac{q^{c}}{(\mathbf{z}_{p})_{hnf}}$$

(7)

Mass transfer (species) equation becomes

$$\frac{\partial C}{\partial t} + u \frac{\partial C}{\partial t} + v \frac{\partial C}{\partial t} = \frac{\partial C}{\partial t} \frac{\partial C}{\partial t} + \frac{D_f}{\rho_{nf}} \frac{\partial T}{\partial t^2} - \frac{kv}{\tau \rho_{nf}} \frac{\partial}{\partial t} [CC_{\infty}]V_T]$$

(8)

The boundary conditions at the plate surface and far into the cold fluid may be written as:

$$x = 0: u_{w}(x), v = 0, \frac{\partial B_{1}}{\partial y} = B_{2} = 0, T = T_{w}, C = C_{w}, \forall y$$

$$x \ge 0: \begin{cases} u_{w}(x) + N\left(1 + \frac{1}{\gamma}\right)\frac{\partial u}{\partial y}, v = 0, \frac{\partial B_{1}}{\partial y} = B_{2} = 0, -k_{nf}\frac{\partial T}{\partial y} = h(T_{w} - T), \\ D_{B}\frac{\partial C}{\partial y} + \frac{D_{T}}{T_{\infty}}\frac{\partial T}{\partial y} = 0 \\ u \to U_{\infty}, T \to T_{\infty}, C \to C_{\infty, aSy \to \infty} \end{cases}$$

$$(9)$$

A. Method of Solution

i. Model simplification.

To seek solution, a stream function $\psi(x, y, t)$ which must identically satisfy continuity equations, such that the stream function $\psi_{u,B}$ corresponding to velocity and magnetic field respectively, satisfies the continuity equation (1) and (2) automatically with

$$u = \frac{\partial \psi_{u}}{\partial y} \text{ and } v = -\frac{\partial \psi_{u}}{\partial x}, \qquad u = \frac{\partial \psi_{B}}{\partial y} \text{ and } v = -\frac{\partial \psi_{B}}{\partial x}$$

$$(10)$$

Similarly a solution of Equations (1) – (4) and (10) and (11) are obtained by defining an independent variable η and dependent variables f and g in terms of the stream function ψ as

$$\eta = y \sqrt{\frac{U_w}{vx(1-at)}}, \psi_u = \sqrt{\frac{v_{wf}xU_w}{1-at}} f(\eta), \qquad \psi_B = \sqrt{\frac{v_{wf}xB_e}{1-at}} g(\eta)$$
(11)

The dimensionless temperature and concentration transformation are given as

$$\theta(\eta) = \frac{T - T_{\infty}}{T_{w} - T_{\infty}} \quad , \qquad \phi(\eta) = \frac{C - C_{\infty}}{C_{w} - C_{\infty}}$$

After a series of simplification the equations become:

Momentum -

$$\left(\frac{\alpha}{c}\frac{\partial}{\partial\eta}(f)(\eta) + \frac{\alpha}{c}\frac{\eta}{2}\frac{\partial^{2}}{\partial\eta^{2}}f(\eta) + \left(\frac{\partial}{\partial\eta}f(\eta)\right)^{2} - f(\eta)\frac{\partial^{2}}{\partial\eta^{2}}f(\eta)\right) = \left(\frac{a}{c}\right)^{2} + \frac{\partial^{3}}{\partial\eta^{3}}f(\eta) - \frac{1-\alpha t}{c}\frac{\sigma B_{o}^{2}(x)}{\rho_{n_{f}}}(f'(\eta)) + \frac{(-\alpha t + 1)^{2}}{c^{2}x}gBc\frac{(C_{w} - C_{\infty})}{\rho_{n_{f}}}\left(\frac{\beta t(T_{w} - T_{\infty})}{\beta c(C_{w} - C_{\infty})}\theta(\eta) + \phi(\eta)\right)$$

Temperature –

$$\frac{\alpha}{c} 2\phi(\eta) + \frac{\alpha \eta}{c} \frac{\partial}{\partial \eta} (\phi(\eta)) + f'(\eta)\phi(\eta) - f(\eta) \frac{\partial}{\partial \eta} (\phi(\eta))$$

$$= \frac{D_m}{\mu_{nf}} \frac{\partial^2}{\partial \eta^2} (\phi(\eta))$$

$$- \frac{k' \nu_{nf}}{\tau \mu_{nf}} \frac{bx}{(1 - \alpha t)^2} \frac{\partial}{\partial \eta} (\phi(\eta)) \frac{\partial}{\partial \eta} \theta(\eta)$$
(13)

With this initial condition below,

$$T \to T_\infty \Longrightarrow T - T_\infty \to 0 \Longrightarrow \theta(\eta) \to 0 \quad (14)$$

$$C \to C_{\infty} \Longrightarrow C - C_{\infty} \to 0 \Longrightarrow \phi(\eta) \to 0$$

We have

$$f'(\eta) = 1 + N \sqrt{\frac{c}{\nu_{nf}(1-\alpha t)}} \frac{\partial}{\partial \eta} (f'(\eta)), f(\eta) = -\frac{\nu_{0}}{\sqrt{\nu_{nf}c}}$$

$$-\frac{k_{nf}}{h} \sqrt{\frac{c}{\nu_{nf}(1-\alpha t)}} \frac{\partial}{\partial \eta} \theta(\eta) = (1-\theta(\eta))$$

$$\frac{\partial}{\partial \eta} (\phi(\eta)) + \frac{D_{T}}{D_{B}T_{x}} \frac{\partial}{\partial \eta} (\theta(\eta)) = 0$$

$$f'(\eta) \to \frac{a}{c}, \theta(\eta) \to 0, \phi(\eta) \to 0$$

$$(15)$$

ii. Solution of model 3 by homotopy analysis method

The HAM is an analytical method which involves obtaining a set of base functions for the representation of the problem at hand. We chose our base functions as $f(\eta)$, $g(\eta)$, and $\theta(\eta)$ because at infinity, the boundary layer flows are decaying exponentially:

$$f(\eta) = a_{0,0}^* + \sum_{k=0}^{\infty} \sum_{n=1}^{\infty} a_{k,n}^* \eta^k e^{-n\eta}$$

$$g(\eta) = b_{0,0}^* + \sum_{k=0}^{\infty} \sum_{n=1}^{\infty} b_{k,n}^* \eta^k e^{-n\eta}$$

$$f(\eta) = c_{0,0}^* + \sum_{k=0}^{\infty} \sum_{n=1}^{\infty} c_{k,n}^* \eta^k e^{-n\eta}$$
(16)

where the $a_{i,k}^*$, $b_{i,k}^*$ and $c_{i,k}^*$ are constants. With the corresponding boundary equations:

$$f'(0,p) = 1 + \lambda_1 \left(1 + \frac{1}{\gamma} \right) f''(0,p), f(0,p) = S, f'(\infty,p) = A$$

$$g''(0,p) = 0, g(0,p) = 0, g'(\infty,p) = 1$$

$$\omega \theta'(0,p) = -(1-\theta), \theta(\infty,p) = 0$$

the general solutions are:

$$f_{d}(\eta) = f_{d}(\eta)' + c_{1} + c_{2}\eta + c_{3}\eta^{2} + c_{4}\eta^{3}$$

$$g_{d}(\eta) = g_{d}(\eta)' + c_{5} + c_{6}e^{\eta} + c_{7}e^{-\eta}$$

$$\theta_{d}(\eta) = \theta_{d}(\eta)' + c_{8}e^{\eta} + c_{9}e^{-\eta}$$
(17)

 $f_d(\eta)'$, $g_d(\eta)'$ and $\theta_d(\eta)'$ are Here, the particular solution, while c's are constants which were determined by the boundary conditions. Lastly, the equations are coded and executed in a symbolic system MAPLE 2021 package. The solution for the non-magnetic case is chosen as an initial guess and the iterations using Euler scheme are continued till convergence within prescribed accuracy is achieved, with the corrections incorporated in subsequent iterative steps until convergence, which is used to obtain the values of our initial guesses. Finally, the resulting guesses together with the system was solved using generalized Thomas' algorithm. The system of equations has to be solved in the infinite domain $0 < \infty < \eta_{\infty}$. A finite domain in the η -direction can be used instead with η chosen large enough to ensure that the solutions are not affected by imposing the asymptotic

conditions finite distance. Gridstudies that independence show the computational domain $0 < \infty < \eta_{\infty}$ can be divided into intervals each of uniform step size which equals 0.02. This reduces the number of points between $0 < \infty < \eta_{\infty}$ sacrificing accuracy. The value $\eta_{\infty} = 5$ was found to be adequate for all the ranges of parameters studied here.

B. Validity of Results

In order to assess the accuracy of the numerical method, we have compared the present results of f''(0) for different values of α with $\beta = 0$ and $\gamma \to \infty$ in the absence of the energy equation versus the previously published data. The comparison is listed in Table 1 and found in excellent agreement.

Table 1: Effect of Flow Governing Parameters on Wall Transfer Rate $f''(\eta)$, $\phi'(\eta)$ and $\theta'(\eta)$

Parameters	$f''(\eta)$	$\phi'(\eta)$	$\theta'(\eta)$	Parameters	$f''(\eta)$	$\phi'(\eta)$	$\theta'(\eta)$
$\lambda = 0.0$	-0.11807	-0.83164	2.07911	$\delta_1 = -0.9$	-0.20811	-0.83626	2.09066
$\lambda = 0.2$	-0.13078	-0.77197	1.92991	$\delta_{1} = -0.3$	-0.17970	-0.81365	2.03413
$\lambda = 0.4$	-0.11655	-0.68183	1.70458	$\delta_1 = 0.3$	-0.13078	-0.77197	1.92991
$\lambda = 0.6$	-0.05649	-0.58595	1.46487	$\delta_1 = 0.9$	-0.34702	-1.00177	2.50442
Ha = 0.1	-0.11025	-0.73524	1.83811	S = -0.4	0.19609	-0.85925	2.14813
Ha = 0.5	-0.18226	-0.88108	2.20270	S = -0.2	0.08497	-0.85220	2.13050
Ha = 1.0	-0.24115	-1.05296	2.63239	S = 0.2	-0.13078	-0.77197	1.92991
Ha = 1.5	-0.27469	-1.20455	3.01138	S = 0.4	-0.23829	-0.70103	1.75258
$\alpha_1 = 0.0$	-0.17966	-0.64642	1.61606	Bi = -0.4	-0.30870	-0.78318	1.95795
$\alpha_1 = 0.3$	0.00989	-1.05408	2.63519	Bi = -0.2	-0.23440	-0.78484	1.96209
$\alpha_1 = 0.6$	0.34924	-1.49296	3.73241	Bi = 0.1	-0.13078	-0.77197	1.92991
$\alpha_1 = 0.9$	-0.09998	-0.04787	0.11966	Bi = 0.4	-0.03907	-0.74601	1.86501
N = 0.0	-0.24739	-0.85658	2.14145	Sr = 0.1	-0.21313	-0.20766	2.07657
N = 0.6	-0.04702	-0.71764	1.79410	Sr = 0.4	-0.13078	-0.77197	1.92991
N = 1.2	0.07806	-0.64555	1.61388	Sr = 0.8	-0.04706	-1.43518	1.79398
N = 2.4	0.25365	-0.56027	1.40068	Sr = 1.4	0.05021	-2.31231	1.65165
Gr = 0.2	-0.25315	-1.33256	3.33140	n = 0	-0.18653	-0.83141	2.07853
Gr = 0.5	-0.13078	-0.77197	1.92991	n = 1	-0.17970	-0.81365	2.03413
Gr = 0.8	0.02196	-0.57012	1.42530	n = 2	-0.17997	-0.81306	2.03264
Gr = 1.5	0.34770	-0.37860	0.94651	n = 3	-0.18109	-0.81356	2.03390
$\beta = 0.0$	-0.17308	-0.80204	2.00510	Sc = 0.30	-0.04147	-0.65080	1.62700
$\beta = 0.3$	0.10822	-0.62851	1.57128	Sc = 0.60	-0.13078	-0.77197	1.92991
$\beta = 0.6$	0.70580	-0.41125	1.02811	Sc = 0.94	-0.17233	-0.81573	2.03932
$\beta = 1.1$	-0.29570	-0.90436	2.26089	Sc = 2.60	-0.22171	-0.84910	2.12274
$N_1 = 0.0$	-0.18609	-0.76628	1.91569	Pr = 0.0015	-0.57632	0.06450	-0.16124
$N_1 = 0.8$	-0.06923	-0.77830	1.94575	Pr = 0.72	-0.13078	-0.77197	1.92991
$N_1 = 1.6$	-0.04256	-0.78105	1.95262	Pr = 4.0	0.44350	-1.65692	4.14231
$N_1 = 3.2$	-0.02404	-0.78296	1.95739	Pr = 6.0	0.74183	-1.88241	4.70602

Table 2: Correlation between the Flow Parameter and the Wall Transfer Rate

Parameters	$f''(\eta)$	$\phi'(\eta)$	$ heta'(\eta)$	
λ				
На	0.77	0.994806	-0.99481	
$lpha_1$	-0.97966	-0.99919	0.999192	
N	0.320564	0.284947	-0.28495	
Gr	0.979312	0.957177	-0.95718	
β	0.999586	0.891218	-0.89122	
δ_1	-0.0668	-0.18761	0.187612	
N_1	-0.51195	-0.58241	0.582414	
S	0.838657	-0.83882	0.838818	
Ві	-0.99998	0.969062	-0.96906	
Sr	0.999168	0.929038	-0.92904	
n	0.993172	-0.99848	-0.98691	
Sc	0.648711	0.776863	-0.77686	
Pr	-0.85292	-0.76977	0.769768	
	0.975296	-0.94304	0.943041	

i. Graphical Results

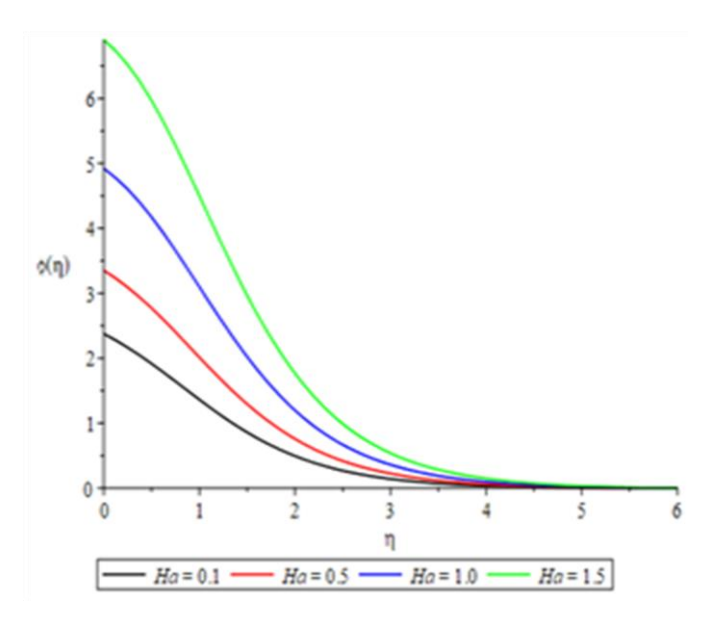


Fig 2.Graph of Chemical Specie for various values stretching parameter *Ha* values stretching parameter.

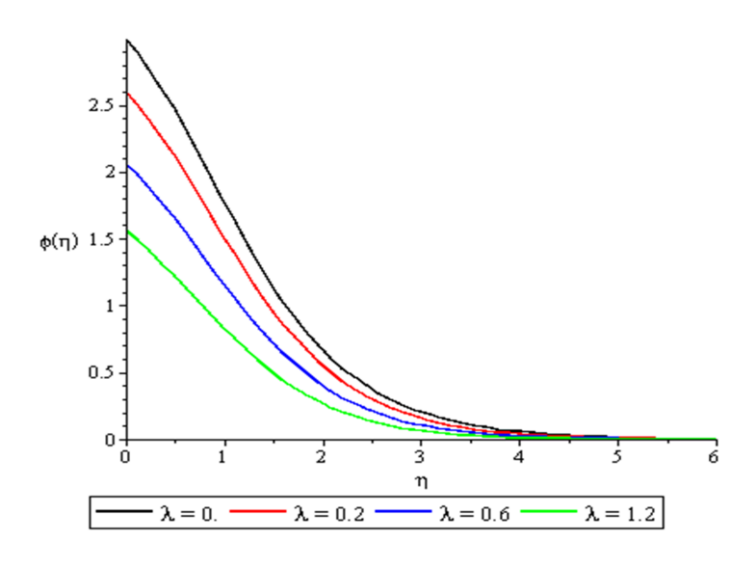


Fig 3.Graph of Chemical Specie for various values stretching parameter λ values stretching parameter

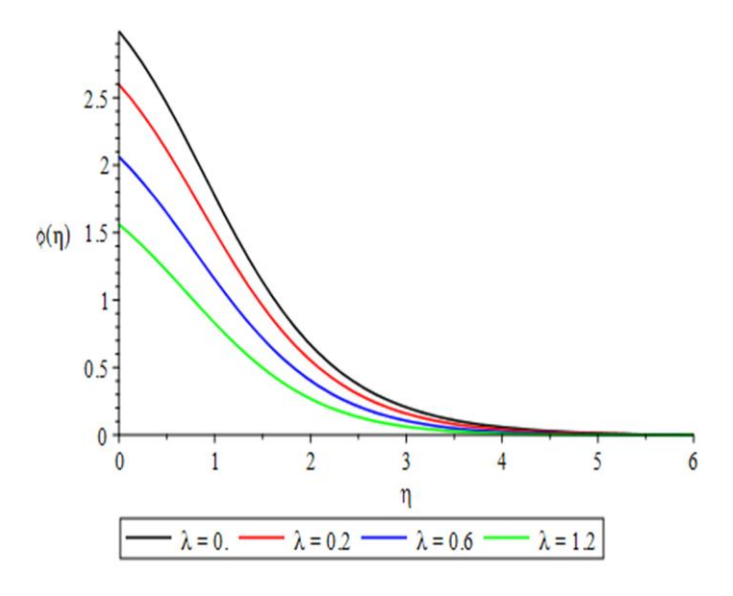


Fig 4. Graph of Chemical Specie for various values stretching parameter λ

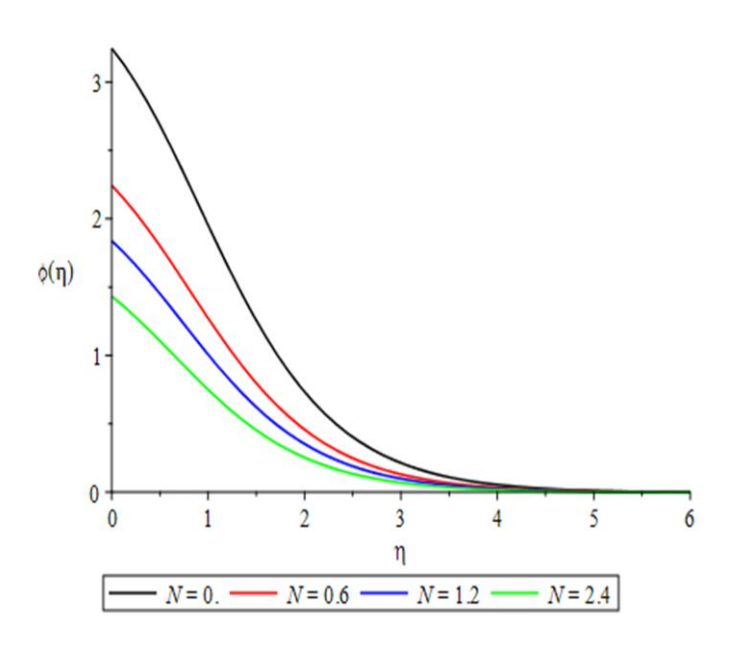


Fig 5.Graph of Chemical Specie for various values stretching parameter *N*

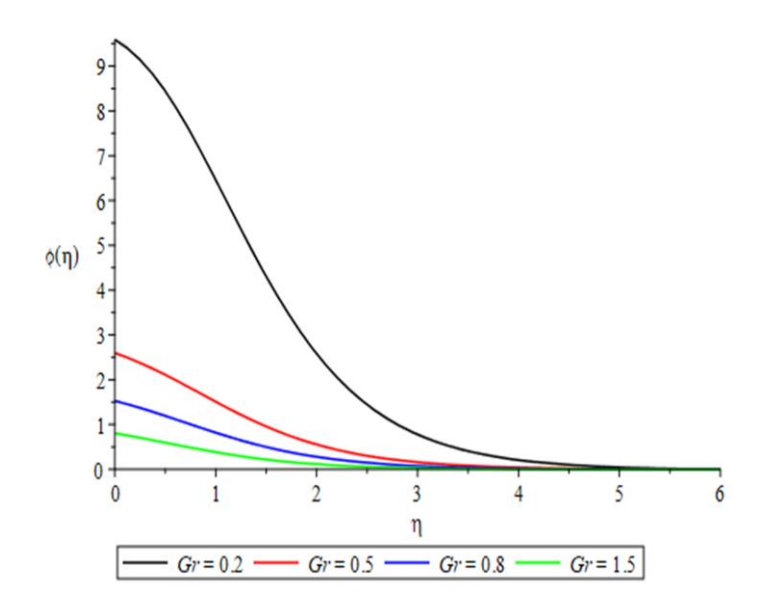


Fig 6.Graph of Chemical Specie for various values stretching parameter *Gr*

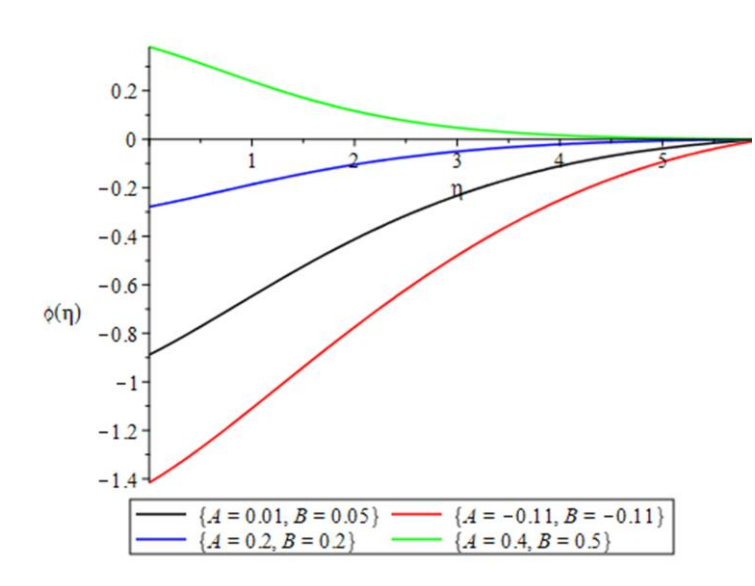


Fig 7. Graph of Chemical Specie for various values stretching parameter *A*, *B*

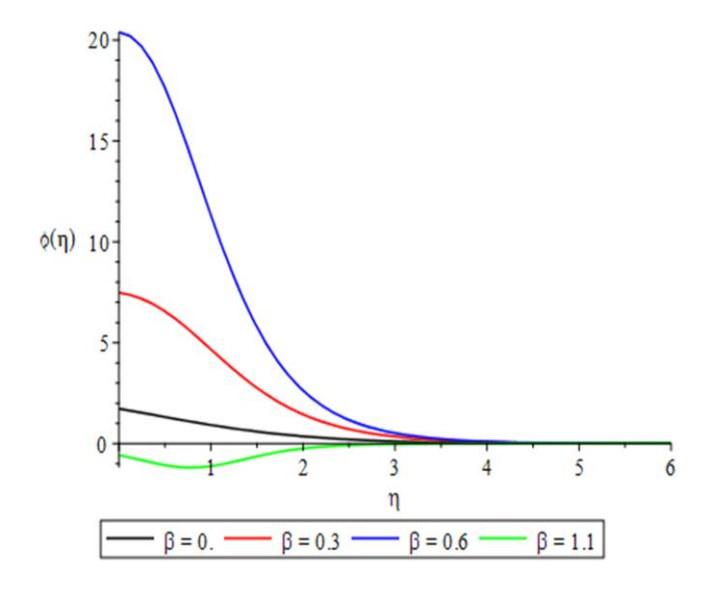


Fig 8. Graph of Chemical Specie for various values stretching parameter β

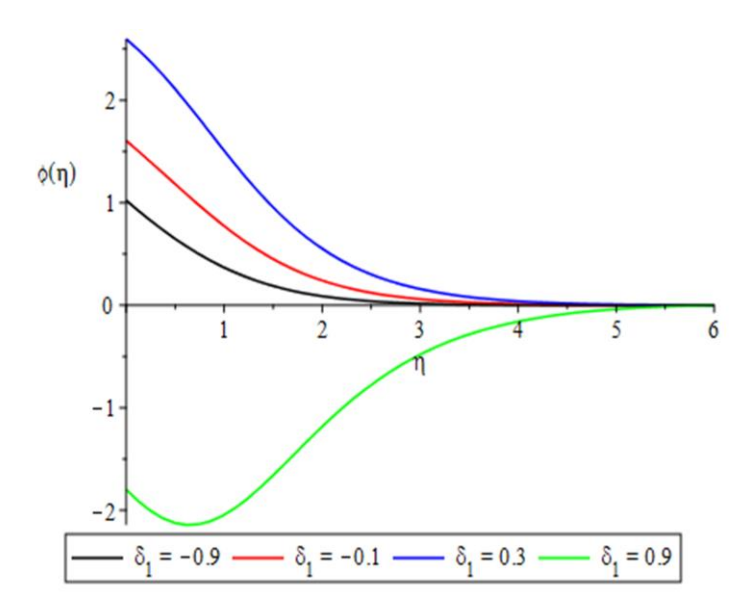


Fig 9. Graph of Chemical Specie for various values stretching parameter δ_1

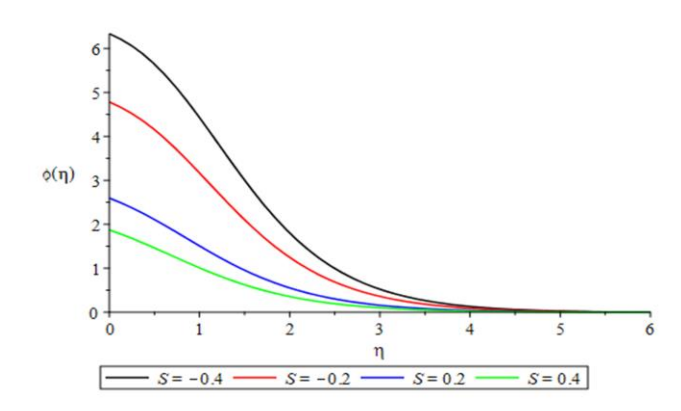


Fig 10. Graph of Chemical Specie for various values stretching parameter S

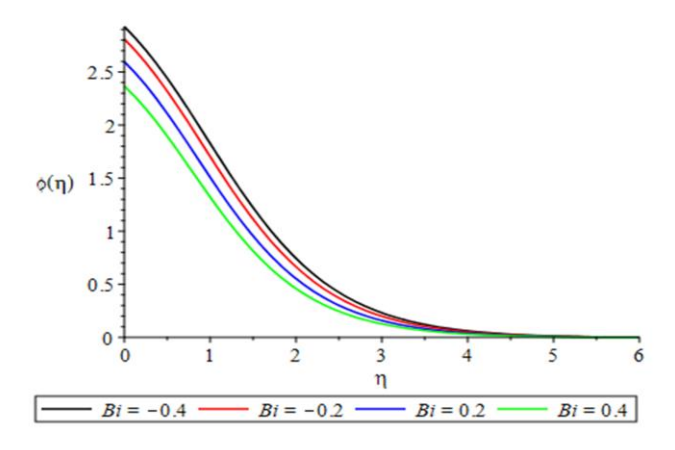


Fig 11. Graph of Chemical Specie for various values stretching parameter B_i

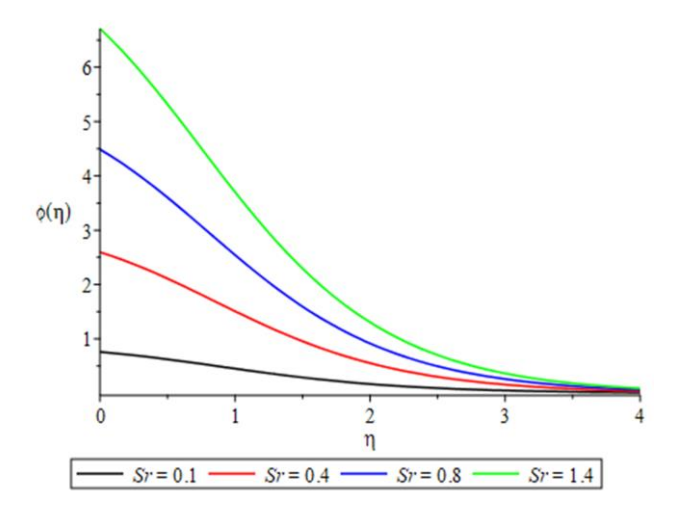


Fig 12. Graph of Chemical Specie for various values stretching parameter *Sr*

III. Discussion and conclusion

The investigation into the significance of multiple slip and induced magnetic fields on unsteady MHD nano-fluid stagnation-point flow over a stretching wedge reveals critical insights into the fluid dynamics of nano-fluids in the presence of external magnetic forces. The analysis highlights the complex interplay between various physical parameters, including slip conditions and magnetic field intensity, which significantly influence the flow characteristics, heat transfer, and boundary layer development. The findings demonstrate that incorporating multiple slip conditions enhance the efficiency of heat transfer and alter the velocity profiles, potentially leading to improved performance in applications such as cooling systems and materials processing. Furthermore, the induced magnetic field plays a pivotal role in stabilizing the flow and can be leveraged to optimize flow control in industrial processes. Overall, this study underscores the importance of considering these factors in the design and optimization of systems utilizing nano-fluids in MHD contexts, paving the way for future research to explore additional parameters and their implications for enhanced fluid performance.

Financial Support

No financial support is obtained in the course of this research

Acknowledgement

Authors acknowledged the tremendous efforts of all anonymous reviewers that will improve this manuscript.

Declaration

The authors of the paper declared that there are no conflicts of interest.

References

- [1] Ali, A. M. & Mohyud-Din, S. T. "Effect of Multiple Slip and Induced Magnetic Fields on MHD Stagnation-Point Flow over a Stretching Wedge." *Journal of Fluid Mechanics*, Volume 885, 2020, A15.
- [2] Bég, O. A. & Zaman, A. "Induced Magnetic Field Effects on MHD Flow and Heat Transfer of Nano-fluids." *Heat Transfer Engineering*, Volume 39, Number 6, 2018, pp583-590.
- [3] Draj, R. R. & Sadeghy, K. "Magnetohydrodynamic Flow of a Nano-fluid over a Stretching Surface."

 Journal of Applied Mechanics and Technical Physics, Volume 51, Number 4, pp. 678-686.
- S. Н., [4] Goh, & Tan, J. K. "Magnetohydrodynamic **Effects** in Nano-fluid Flow Stretching Over Surfaces." Applied Thermal Engineering, Volume 197, 2021, pp 117523.
- [5] Hossain, M. A. & Gafur, M. A. (2011). "MHD Flow of a Nano-fluid over a Stretching Surface with Variable Thermal Conductivity." *Journal of Nano-fluid Science*, Volume 1, Number 2, 2011, pp. 97-106.
- [6] Hussain, M., et al. "Effects of Multiple Slip Conditions on the Stagnation Point Flow of a Nano-fluid." *Journal of Molecular Liquids*, Volume 218, 2016, pp. 464-470.
- [8] Khan, W. Q. & Pop, I. "Boundary Layer Flow of a Nano-fluid Past a Stretching Sheet." *Chemical Engineering Research and*

- Design, Volume 88, Number 9, 2010, pp.1170-1175.
- [9] Kumar, R., & Singh, R. "Unsteady MHD Flow of Nano-fluids with Multiple Slip Conditions: A Review." *Journal of Molecular Liquids*, Volume 348, 2022, pp. 118008
- [10] Mahmoud, S. R., & Mahmoud, A. H. "Effects of Magnetic Field on Unsteady MHD Nano-fluid Flow over a Stretching Surface with Heat Transfer." *International Journal of Numerical Methods for Heat & Fluid Flow*, Volume 25, Number 5, 2015, pp. 1258-1274.
- [11] Nadeem, S. & Lee, H.

 "Magnetohydrodynamic Flow of a
 Nano-fluid with Thermal Radiation over
 a Stretching Surface." *Journal of Engineering Mathematics*, Volume 83,
 Number 3, pp. 453-467.